THE PERFORMANCE OF A TIGHT INS/GNSS/PHOTOGRAMMETRIC INTEGRATION SCHEME FOR LAND BASED MMS APPLICATIONS IN GNSS DENIED ENVIRONMENTS

Chien-Hsun Chu [a,] *, Kai-Wei Chiang [b]

[a] Dept. of Geomatics, National Cheng Kung University, Taiwan – chienhsun0229@msn.com
[b] Department of Geomatics, National Cheng-Kung University, Taiwan – kaiwei.chiang@gmail.com

Commission ICWG I/Va

KEY WORDS: Direct georeferencing, Constraint, Mobile Mapping System, Control points

ABSTRACT:

The early development of mobile mapping system (MMS) was restricted to applications that permitted the determination of the elements of exterior orientation from existing ground control. Mobile mapping refers to a means of collecting geospatial data using mapping sensors that are mounted on a mobile platform. Research works concerning mobile mapping dates back to the late 1980s. This process is mainly driven by the need for highway infrastructure mapping and transportation corridor inventories. In the early nineties, advances in satellite and inertial technology made it possible to think about mobile mapping in a different way. Instead of using ground control points as references for orienting the images in space, the trajectory and attitude of the imager platform could now be determined directly. Cameras, along with navigation and positioning sensors are integrated and mounted on a land vehicle for mapping purposes. Objects of interest can be directly measured and mapped from images that have been georeferenced using navigation and positioning sensors. Direct georeferencing (DG) is the determination of time-variable position and orientation parameters for a mobile digital imager. The most common technologies used for this purpose today are satellite positioning using the Global Navigation Satellite System (GNSS) and inertial navigation using an Inertial Measuring Unit (IMU). Although either technology used along could in principle determine both position and orientation, they are usually integrated in such a way that the IMU is the main orientation sensor, while the GNSS receiver is the main position sensor. However, GNSS signals are obstructed due to limited number of visible satellites in GNSS denied environments such as urban canyon, foliage, tunnel and indoor that cause the GNSS gap or interfered by reflected signals that cause abnormal measurement residuals thus deteriorates the positioning accuracy in GNSS denied environments. This study aims at developing a novel method that uses ground control points to maintain the positioning accuracy of the MMS in GNSS denied environments. At last, this study analyses the performance of proposed method using about 20 check-points through DG process.

1. INTRODUCTION

The development of land-based mobile mapping systems was initiated by two research groups, namely The Center for Mapping at Ohio State University, USA, and the Department of Geomatics Engineering at the University of Calgary, Canada. In the early 2000s, a number of land-based Mobile Mapping Systems (MMS) have been utilized in commercial applications (Chiang et al., 2008). The process of mobile mapping involves producing multiple images of a given object from various positions. The three-dimension (3D) positions of the object with respect to the camera frame can then be measured. An Inertial Navigation System (INS) is a self-contained navigation technique in which measurements provided by accelerometers and gyroscopes are used to track the position and orientation of an object relative to a known starting point, orientation and velocity. The Global Navigation Satellite Systems (GNSS) is a universal, all-weather, world-wide positioning system that provides time, position, and velocity data. Both systems can be used as stand-alone navigation tools or in conjunction with other sensors for various purposes. Moreover, the integration of GNSS and INS can overcome problems with environments such as urban canyons, forests, and indoor settings, where GNSS alone cannot provide service. In order to attain reasonable accuracies of position and orientation solutions, a tactical grade or higher quality INS along with GNSS has been applied as the primary position and orientation system for current commercial systems.

In the classical approach, the Kalman Filter (KF) is applied in real-time applications to fuse different data from various sensors while optimal smoothing is applied in the post-mission mode. The basic idea of using the KF in INS/GNSS integration is to fuse independent and redundant sources of navigation information with a reference navigation solution to obtain an optimal estimate of navigation states, such as position, velocity and orientation. The Figure 1 illustrates typical positional error accumulation of KF during GNSS outages. In fact, the error behaviour of orientation parameters during GNSS outages is similar to positional error shown in the Figure 1. The scale of the maximum positional drift shown in Figure1 is given based on the average value of the Microelectromechanical System Inertial Measurement Unit (MEMS IMU) (Gyro bias 100 deg/hr). Unfortunately, GNSS outage takes place frequently in modern urban canyon even if indoor. The magnitudes of the positional and orientation errors depend on the quality of the inertial sensors, the length of GNSS outage, the dynamics of vehicle and the effectiveness of the algorithms applied. In other

* Corresponding author: C.H. Chu

words, proper modification of inertial sensors or sensor fusion algorithms can reduce the magnitude of accumulated positional and orientation error during frequent GNSS outages (Chiang, et al., 2011). Therefore, the goal of developing an alternative INS/GNSS integration scheme is to reduce the impact of remaining limiting factors of KF and improve the positioning accuracy during GNSS outages which is critical for land based mobile mapping applications.

Optimal smoothing algorithms, also known as smoothers, have been applied for the purpose of accurate positioning and orientation parameter determination through post-processing for most of surveying and mobile mapping applications with integrated sensors. In contrast to the KF, the smoothing is implemented after all KF estimates have been solved by the use of past, present and future data. As shown in Figure1, the magnitudes of positional and orientation errors during GNSS outage can be improved significantly after applying one of these optimal smoothing algorithms. However, the magnitude of residual error shown with blue line also depends on the quality of the inertial sensors, the dynamics of vehicle and the length of GNSS signal outage. Therefore, the reduction of remaining positional and orientation errors becomes critical when integrating a low cost MEMS IMU with GNSS for land based mobile mapping applications.

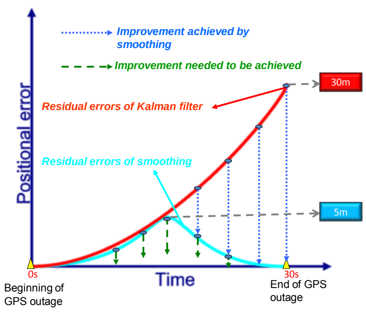

Figure 1: The KF's positional error behaviour during GNSS outage

The idea of mobile mapping is basically executed by producing more than one image that includes the same object from different positions, and then the 3D positions of the same object with respect to the mapping frame can be measured (Tao and Li, 2007). Multi-platform and multi-sensor integrated mapping technology has clearly established a trend towards fast geospatial data acquisition. Sensors can be mounted on a variety of platforms, such as satellites, aircraft, helicopters, terrestrial vehicles, water-based vessels, and even people. As a result, mapping has become mobile and dynamic. In the words, mobile mapping refers to a means of collecting geospatial data using mapping sensors that are mounted on a mobile platform.

The core technology of MMS is Direct-Georeferencing (DG) that can get 3D coordinate of object without Ground Control Points (GCPs). Equation (1) and Figure 2 illustrate the general concept of the DG. With this implementation, the coordinates of a mapping feature can be obtained directly through measured image coordinates. This procedure works based on the a priori knowledge of various systematic parameters, as shown in the following expression (Chu, et al., 2013):

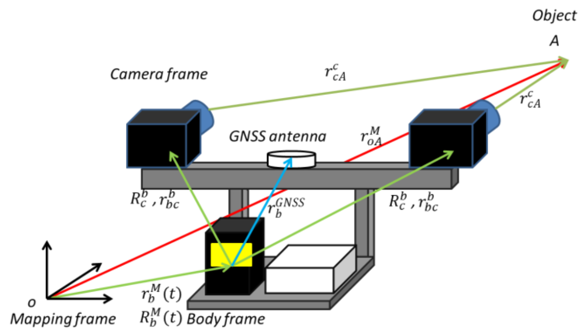

Figure 2: The concept of DG

$$r^M_{oA} = r^M_{ob}(t) + R^M_b(t)(r^b_{bc} + sR^b_c r^c_{cA}) \quad (1)$$

Where,

r^M_{oA} = the position vector of an object in the chosen mapping frame

$r^M_{ob}(t)$= the position vector of INS/GNSS in the m frame at time (t)

r^c_{cA} = the vector of image coordinates given in the c-frame

r^b_{bc} = the lever arm vector which is from the body frame to the camera frame

r_b^{GNSS} = the lever arm vector between INS and GNSS antenna

$R^M_b(t)$= the 3-D transformation matrix which rotates the body frame (or INS frame) into m-frame

R^b_c = the boresight transformation matrix which rotates the camera frame into body frame

s = a scale factor specific to a one-point/one-camera combination which relates the image coordinates to the object coordinates

The elements of r^c_{cA} is obtained from measuring image coordinates; s is determined by the stereo techniques; $R^M_b(t)$ and $r^M_{ob}(t)$ are interpolated from INS/GNSS integrated POS at the exposure time (t); those elements are known. The vector between the phase centre of the GNSS antenna and the centre of INS (r_b^{GNSS}) is an unknown parameter, but it is determined through a surveying process. The calibration process must be conducted prior to operate MMS. Those procedures include lever arm and boresight calibration, that determine r^b_{bc} and R^b_c individually.

Before performing calibration procedure, the sufficient quantity of GCPs has been estimated. Then the lever arm and boresight parameters can be derived through the bundle adjustment. Therefore, the top priority is to establish a ground control field with sufficient accuracy after the implementation of proposed MMS hardware architecture. A two-step approach to conduct the lever arm and the boresight for system calibration is applied in this study. The image acquisition is performed at the ground calibration field, and the measurements of the image points are also processed at this stage. The Australis software is used to calculate the EOPs of those images through the bundle adjustment. After performing the interpolation of INS/GNSS data at the image exposure time, the differences of the position and the attitude between the Exterior Orientation Parameters (EOPs) and the interpolated INS/GNSS data are applied.

In the process of the lever arm calibration, the perspective position of each image (r^M_{oc}) is exactly known after the bundle adjustment, and the calculation about the INS/GNSS position vector (r^M_{ob}) is conducted by the interpolation at the same time.

Then the lever arms (r^b_{bc}) can be solved by the following equation (Li, 2010):

$$r^b_{bc} = R^b_M(r^M_{oc} - r^M_{ob}) \quad (2)$$

In the aspect of the boresight calibration, the rotation matrix between the camera frame and the mapping frame of each image (R^M_c) is also obtained from the bundle adjustment results, and the rotation matrix between the body frame and mapping frame of each image can be measured by INS. Eventually, the rotation matrix (R^b_c) can be calculated by the matrix multiplication (Li, 2010):

$$R^b_c = R^b_M R^M_c \quad (3)$$

Generally speaking, the accuracy of the calibration process is dominated by the quality of the INS/GNSS data and the bundle adjustment results. This relationship also affects the performance of MMS indirectly. In this case, the distribution of the control points in the image and the quality of the INS/GNSS data are very important during the calibration process. After obtaining calibration parameters, the DG task can be performed exactly works without GCPs.

2. PROBLEM STATMENTS

In order to achieve high accuracy for positioning and orientation determination in mobile mapping applications, the measurements are processed in post-mission mode with an optimal smoothing algorithm. Most of the commercial mobile mapping systems use an optimal smoothing algorithm to provide accurate information on position and orientation for DG (El-Sheimy, 1996). However, commercial INS/GNSS integrated systems use tactical grade IMUs or above to provide accurate solutions for general mobile mapping applications. Therefore, upgrading the hardware (e.g., IMU) can be considered as an effective solution to improve the accuracies of position and orientation parameters when a low cost MEMS IMU is used. Another effective way to improve the accuracies of low cost MEMS INS/GNSS integrated solutions is through the improvement of sensor fusion algorithms. Figure 3 illustrates the loosely coupled (LC) INS/GNSS integration scheme commonly applied by most of the commercial mobile mapping systems (Titterton, and Weston, 1997; Brown and Hwang, 1992).

The process of the KF is divided into two groups, those for prediction and updating. The time prediction equations are responsible for the forward time transition of the current epoch (k-1) states to the next epoch (k) states. The measurement update equations utilize new measurements into the prior state estimation to obtain an optimized posteriori state estimation. The update engine of KF is triggered at every GNSS measurement using the difference between GNSS and INS solutions as input. Hence, the KF generates an updated estimate for reducing the INS errors using measurement update equations. Whenever GNSS measurements are not available, the KF works in the time prediction mode to estimate the error state vector. The optimal smoothing is performed after the filtering stage and thus it relies on the previously filtered solutions. Consequently, an accurate filtering procedure is required for accurate smoothing process (Brown and Hwang, 1992; Gelb, 1974). A fixed-interval smoother, the Rauch-Tung-Striebel backward smoother is implemented in this study. In fixed-interval smoothing, the initial and final time epochs of the whole period of measurements (i.e. 0 and N) are fixed. Compared to other fixed-interval smoothers, the Rauch-Tung-Striebel backward smoother has the advantage of being the simplest to implement (Brown and Hwang, 1992; Gelb, 1974). It consists of a forward sweep and a backward sweep. The forward sweep is the common KF with all predicted and updated estimates and corresponding covariance saved at each epoch of the whole mission. The backward sweep begins at the end of the forward filter (i.e. at epoch N), see (Brown and Hwang, 1992; Gelb, 1974) for details. The smoothed estimates at any epoch k are computed as a linear combination of the filtered estimate at that epoch and the smoothed estimate at the heading epoch k+1. Thus, these smoothed estimates can be considered as updating the forward filtered solution to obtain improved estimates. The computation of the smoothed estimates at each epoch requires the storage of the KF predicted and updated (filtered) estimates and their corresponding covariance at each epoch (Brown and Hwang, 1992; Gelb, 1974). This is the case in INS/GNSS integrated solutions when uninterrupted GNSS data streams are available. During GNSS outages, only predicted estimates and covariance are available, a post-mission smoother can significantly remove the residual errors of KF (Titterton, and Weston, 1997; Brown and Hwang, 1992); however, some residual errors still remain, as shown in Figure1. Therefore, the error behaviour shown in Figure1 motivate various studies concerning the development of alternative multi-sensor fusion algorithms to reduce the magnitude of accumulated positional and orientation errors during frequent GNSS outages in land applications.

The Figure 3 shows loosely coupled strategy. This kind of integration has the benefit of a simpler architecture which is easy to utilize in navigation systems. However, the errors in the position and velocity information provided by the GNSS KF are time-correlated, which can cause degradation in performance or even instability of the navigation KF, if these correlations are not considered by some means. In the case of incomplete constellations, i.e. less than four satellites in view, the output of the GNSS receiver has to be ignored completely, leaving the INS unaided. Therefore, the current loosely coupled INS/GNSS integration architecture is not suitable for land mobile mapping applications where frequent and long GNSS outages are anticipated to deteriorate the performance of DG significantly.

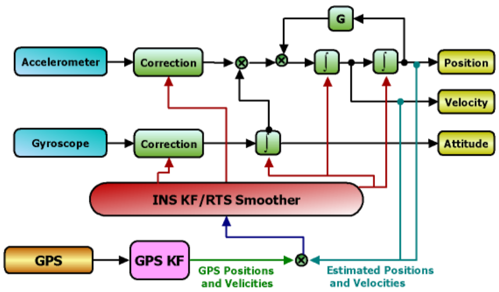

Figure 3: The integration architecture of LC (closed loop)

The tightly coupled INS/GNSS integration architecture uses a single KF to integrate GNSS and IMU measurements. Figure 4 describes the TC integration architecture. It shows that raw measurements are collected from the IMU and are converted to position, velocity and attitude measurements in the desired coordinate system using the INS mechanization algorithms. In the TC integration architecture, the GNSS pseudo-range, delta-range and carrier phase measurements are processed directly in the main Kalman filter (Hide and Moore, 2005). The aiding of the receiver tracking loops using velocity information provided by the INS is an essential characteristic of a tightly coupled system, too. The primary advantage of this integration is that raw GNSS measurements can still be used to update the INS when less than four satellites are available. This is of special benefit in a hostile environment such as downtown areas where the reception of the satellite signals is difficult due to obstruction. In addition, in the case when carrier phase GNSS measurements are used, the IMU measurements will be used to aid the ambiguity resolution algorithm. However, the TC integration architecture is not commonly used to integrate GNSS and INS simply because of its additional complexity over the LC approach. As shown in Figure 5, the positioning accuracies of TC and LC architectures remain similar when the number of visible satellite is larger than four. However, the accuracy of LC architecture decrease significantly when the number of visible satellite become less than four. On the contrary, the accuracy of TC architecture remains stable when the number of visible satellite becomes less than four. However, the accuracy of TC architecture starts to decrease when the number of visible satellite becomes less than two. Although TC architecture seems to be a better candidate for land based mobile mapping applications, but TC architecture still suffer the impact of frequent GNSS signal blockage in urban area. The GNSS signal visibility and quality still play a vital role when applying TC architecture for land based mobile mapping applications. Of course none of those issues would matter when expensive and controlled navigation grade IMUs are available to general users, however, those issues are the key to improve the quality of track with the TC architecture for land mobile mapping applications using current commercially available tactical grade IMU.

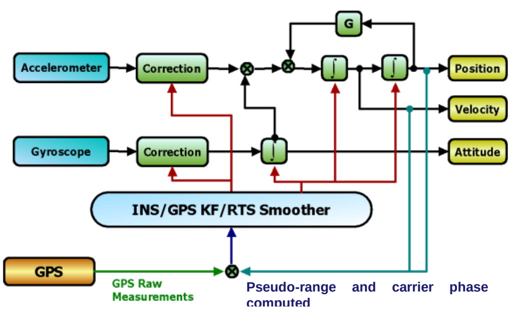

Figure 4: The integration architecture of TC (closed loop)

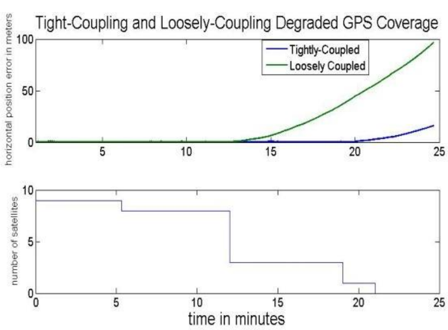

Figure 5: The comparison between TC and LC architectures with variable number of visible satellite

Above mention, there are two main algorithms LC and TC to integrate INS/GNSS for quality of track so far. On the other hand, some commercial software also has the other method for quality control. They are supposed to control point throughout the whole area. They convert and correct Point of Interesting (POI) through bundle adjustment after finishing the whole work. This method needs much time because it processes the whole data. The objective of this study is that quickly gets updated information through the photogrammetry technology to correct track in GNSS outage area. The error of track can be controlled by this method during GNSS outage. This study proposes a MMS cart developed at the National Cheng Kung University (NCKU) in Taiwan to verify DG capability with the photogrammetry technology aiding.

3. THE CONFIGURATIONS OF PROPOSED MMS

The Figure 6 shows a prototype MMS cart which is developed by NCKU. This MMS cart is designed for situations of indoor or GNSS outages area that is divided into sensor's frame and cart. All sensors are fixed on a frame for keeping on relative location and attitude, which can be adjustable for view of height. The main sensors are Positioning and Orientation System (POS), which is iNAV-RQH-10018-iMAR and panoramic camera, which is Ladybug5. Their specifications are shown in the Figure7 and Figure 8. The other hardware, like computer and power supply, is designed to fix on the cart. The iNAV-RQH-10018-iMAR is a navigation grade Inertial Navigation System (INS) that uses laser gyro and dual-frequency GNSS receiver. The Ladybug5 is a panoramic camera that has high resolution and 90% of full sphere view angle. They are good choice for frequent GNSS outage area even if indoor.


Figure 6: The proposed MMS cart

Volume	29.9x21.3x17.9 (cm³)	
Weight	9 Kg	
I/O Interface	Ethernet TCP/IP / UDP	
	gyro	accelerometer
Bias drift	<0.002 deg/hr	<25μg
Scale factor	< 5 ppm	< 100 ppm
Random Walk	0.0015 °/√h	< 8 μg/√(Hz)
misalignment	< 25 μrad	

Figure 7: The specification of proposed INS

Diameter :	19.7 (cm)
Height:	16 (cm)
Weight	3 Kg
I/O Interface	USB 3.0
Focal length	4.4 mm
shutter	Global shutter 0.2~2 sec
View angle	90% of full sphere
Pixel size	3.45 µm
Max. Resolution	2048x2448

Figure 8: The specification of proposed camera

We also develop a set of mapping software called "PointerMMS", which has two main functions that are system calibration and measuring of POI. On the aspect of system calibration, the PointerMMS can calculate system calibration parameters that are lever-arm and boresight using two-step method, after loading track and EOPs of images. On the other hand, the PointerMMS can be not only load track and images but also dose DG for measuring of POI. In this study, we develop a control point feedback method that can use simple photogrammetric method to quickly correct track and ascend accuracy of POI. The details are illustrated in next theme. In this study, the MMS cart is calibrated by the PointerMMS in a control field at NCKU campus. The control field is built by traditional surveying method that has over 100 3D control points and check points whose accuracy are about 2 cm. The Figure 9 shows the calibration experiment. In the Figure 9, pink points are control points, yellow points are cameras and green triangles present position and heading of POS. The accuracy of system calibration of MMS cart is shown in the Table 2. The lever arm relationship is around 8 cm and the boresight angle's accuracy is about 0.18 degree. After derivation, that causes about 6 cm error for 20 m objects.

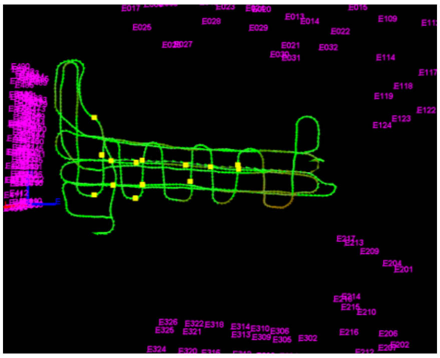

Figure 9: Calibration experiment of MMS cart

Table 2: The calibration accuracy of every camera

STD	Lever-Arm (m)			Boresight (deg.)		
	X	Y	Z	Omega	Phi	Kappa
Cam1	0.044	0.075	0.021	0.147	0.141	0.141
Cam2	0.048	0.073	0.021	0.174	0.076	0.174
Cam3	0.044	0.075	0.024	0.150	0.113	0.153
Cam4	0.044	0.074	0.022	0.155	0.116	0.152
Cam5	0.046	0.085	0.022	0.178	0.076	0.177

After obtaining calibration parameters, the DG task can be performed exactly works without GCPs. The MMS cart also does DG accuracy verification through check fields. The Figure 10 shows track of DG accuracy verification experiment and check points. The object distance is about 7 meter when MMS cart dose DG accuracy verification.

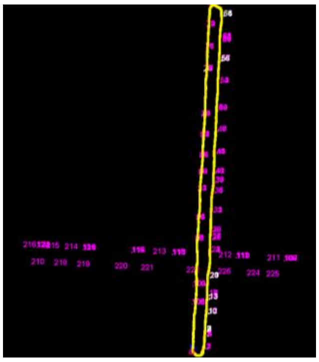

Figure 10: DG accuracy verification experiment of MMS cart

The Figure 11 shows measuring POIs in PointerMMS for DG accuracy verification and the Table 3 illustrates the DG accuracy of the MMS cart. In other word, the MMS cart has less than 12 cm 3D error in 7 meter object distance.

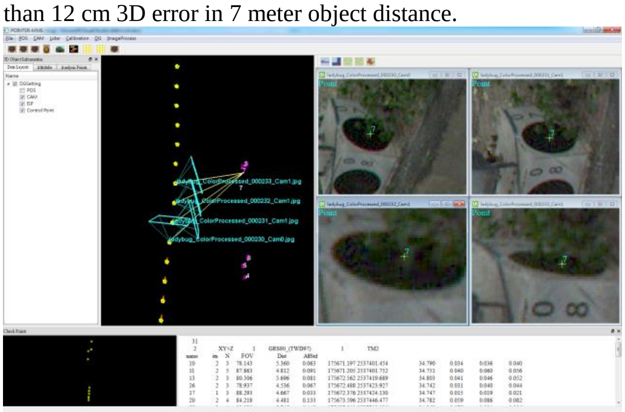

Figure 11: Measuring POIs and PointerMMS interface

Table 3: DG accuracy of the MMS cart

	Number: 31				
(meter)	E	N	H	2D	3D
AVG	0.011	-0.035	-0.041	0.036	0.055
STD	0.078	0.06	0.036	0.099	0.105
RMS	0.078	0.068	0.054	0.104	0.117

4. THE INTEGRATION OF PHOTOGRAMMETRY/INS/GNSS

Although the INS/GNSS integration system is able to perform seamlessly during GNSS outage, the accuracy degrades with GNSS outage time. In addition, frequent and long GNSS outages taking place in typical urban canyon degrade the accuracy of POS applied by the land based MMS thus deteriorate the accuracy of DG operation significantly. In order to restrain the weakness, this study provides a method called control point feedback that takes advantage of control points updating POS solution through photogrammetry technology. This method is believed that can significantly descend error in GNSS outage area. The Figure 12 shows the estimated error behaviour of pure INS smooth track and control point feedback smooth track in GNSS outage.

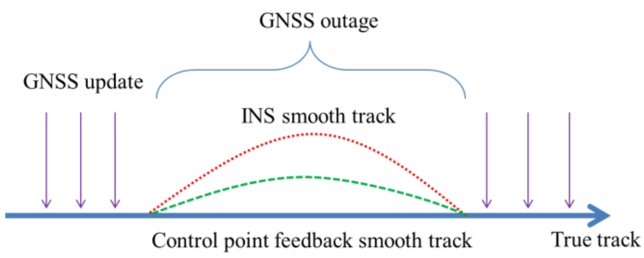

Figure 12: The estimated error of tracks

The control point feedback uses resection of single image and measures more than 3 control points to solve the EOPs of the image. The EOPs of each image can derive position and attitude of responded epoch of track through system calibration parameters. At last, this study sets a period of each image for smoothing. The Figure 13 illustrates the process of control point feedback that is the computed EOP by resection of each image and smoothing during GNSS outages.

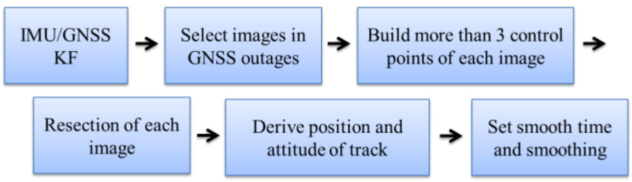

Figure 13: The process of control point feedback

The Figure 14 illustrates EOPs are derived to the position and attitude of IMU (Chu and Chiang, 2012). In the derivation process, the attitude of image and boresight angle are converted to rotation matrix by Direction Cosine Matrix (DCM) for multiplication at first. In this step, it gets rotation matrix R_m^b from mapping frame to body frame. In other words, it is the rotation matrix between IMU frame and mapping frame. In the second step, because the IMU frame is supposed to the completely overlapping with mapping frame, the lever-arm frame is converted to mapping frame by the rotation matrix R_b^m, and then the IMU position can be calculated by the position of image adding the converted lever-arm in the same coordinate system at the last step.

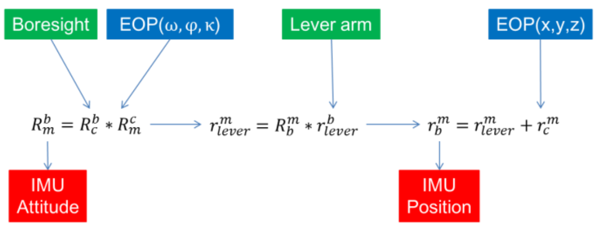

Figure 14: The detail of derivation

The EOPs of each image can be quickly solved by resection using more than 3 control points and then are derived into IMU position and attitude by lever-arm and boresight. Because the control points can be measured by other surveying methods in GNSS outage area and the derived position and attitude are corrected and smoothed track, the accuracy can be significantly ascended during GNSS denied environment.

5. RESULTS AND DISCUSSIONS

This study aims at the performance between control point feedback and pure INS smooth during GNSS outage area. This study designs a route start point from outdoor into indoor and then come back start point. The Figure15 shows the route whose red part is in indoor area about 10 minutes. There are some 3D control points and check points that are pink points along track.

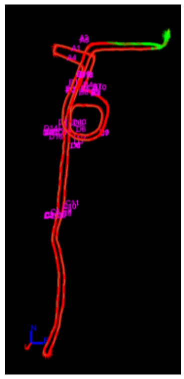

Figure 15: The track of DG verification of control point feedback

This study measures some check points through DG based on control point feedback or not used. The Figure 16 whose blue line illustrates corrected shift shows the detail of correction. The Table 4 and Table 5 illustrate the accuracy of them. The Table 4 shows that has about 5 meter error of POI in 3D at average 8 meter between MMS cart and objects without control point feedback. On the other hand, the Table 5 shows the accuracy of POI that is ascended to 0.5 meter in 3D at the same distance with control point feedback. After estimation, the control point feedback can ascend the accuracy of POI about 5~10 times shown in the Table 6.

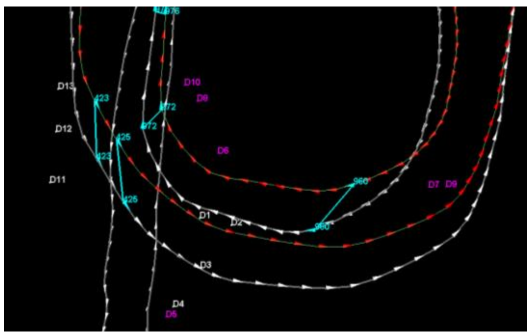

Figure 16: The detail of control point feedback correction

Table 4: The error of POI without control point feedback

		Number:	18		
(meter)	E	N	H	2D	3D
AVG	2.7	1.387	-0.638	3.035	3.102
STD	3.453	0.96	1.066	3.584	3.739
RMS	4.307	1.671	1.217	4.62	4.777

Table 5: The error of POI with control point feedback

		Number:	24		
(meter)	E	N	H	2D	3D
AVG	0.016	-0.076	0.001	0.078	0.078
STD	0.283	0.266	0.137	0.388	0.412
RMS	0.278	0.271	0.134	0.388	0.41

Table 6: The rate of progress

100%	E	N	H	2D	3D
RMS	14.49	5.17	8.08	10.91	10.65

6. CONCLUSIONS

This study develops an MMS Cart that is enough to be applied on DG. Its lever arm relationship is around 2 cm and its boresight angle's accuracy is about 0.18 degree. In other words, that causes about 6 cm error for 20 m objects. This study aims at special situation like canyon, foliage, tunnel or indoor to develop control point feedback method for keeping on quality of track. The control point feedback method uses a simple and quick photogrammetry method to correct and smooth track. In the final experiment, this study verifies DG performance of the MMS cart in indoor environment, comparing with control point feedback aiding or not. The DG accuracy of the MMS is about 5 m during 10 minutes GNSS outage at average 8 meter between MMS cart and objects without control point feedback aiding. Fortunately, the DG accuracy can be ascended 5~10 times to about 0.5 meter with control point feedback method.

ACKNOWLEDGEMENTS

The authors would acknowledge the financial supports provided by the Department of land administration, Ministry of Interior of the Executive Yuan, R.O.C. (Taiwan).

The authors would acknowledge the funds of travel provided Ministry of Science and Technology, R.O.C. (Taiwan).

REFERENCES

Brown, R.G. and Hwang, P.Y.C. 1992. Introduction to random signals, John Wiley and Sons, New York.

Chiang, K.W. Noureldin, A. and El-Sheimy, N. 2008. Developing a Low Cost MEMS IMU/GNSS Integration Scheme Using Constructive Neural Networks, IEEE Transactions on Aerospace and Electronic Systems,44(2): 582-594

Chiang, K.W., Chang, H.W. Li, C.Y. and Huang, Y.W. 2011. An ANN embedded RTS smoother for an INS/GPS integrated Positioning and Orientation System, *Applied Soft Computing.* 11(2): 2633-2644

Chu, C.H. Chiang, K.W. and Lin, C.A. 2013. The Performance Analysis of a Portable Mobile Mapping System with Different GNSS Processing Strategies, ION GNSS 2013, Nashville, USA.

Chu, C.H. and Chiang, K.W. 2012. The Performance of a Tight INS/GNSS/PHOTOGRAMMETRIC Integration Scheme for Land Based MMS Applications in GNSS denied environment, The XXII Congress of the International Society for Photogrammetry and Remote Sensing, Melbourne, Australia.

El-Sheimy, N. 1996. The development of VISAT - A mobile survey system for GIS applications. Ph.D. thesis, UCGE Report No. 20101, Department of Geomatics Engineering, the University of Calgary: Calgary, Canada.

Gelb, A. 1974. Applied Optimal Estimation, The Analytic Science Corporation.

Hide, C. and Moore, T. 2005. GNSS and Low Cost INS Integration for Positioning in the Urban Environment, Proc. of ION GNSS 2005, pp.1007-1015

Li, Y.H. 2010. The Calibration Methodology of a Low Cost Land Vehicle Mobile Mapping System, ION GNSS 2010, Portland, OR

Tao, V. and Li, J. (2007): Advances in Mobile Mapping Technology; International Society for Photogrammetry and Remote Sensing (ISPRS) Book Series; Taylor and Francis Group: London, UK.

Titterton, D. H. and Weston, J. L. 1997. Strapdown Inertial Navigation Technology. Peter Peregrinus Ltd